

ENCLOSURE 2

SEQUOYAH NUCLEAR PLANT (SQN),

UNIT 2 CYCLE 5

RESTART PHYSICS TEST SUMMARY

(PFE-G22NP)

NONPROPRIETARY

PFE-G22NP

Sequoyah Nuclear Plant
Unit 2, Cycle 5
Restart Physics Test Summary

Nuclear Fuel
PWR Fuel Engineering

January 1991

Prepared by *John David Waters* Date *1-18-91*
Approved by *[Signature]* Date *1-22-91*

ABSTRACT

The Sequoyah Nuclear Plant Unit 2, Cycle 5 Restart Physics Test Summary covers the period from September 21, 1990 through December 31, 1990. The report presents restart physics test results and operational data for the first 32 effective full-power days (EFPD). The tests included are initial criticality, primary coolant critical boron concentration, reactivity control, isothermal temperature coefficient, and power distribution measurements.

The results in this report have been verified in accordance with Nuclear Fuel Instructions.

John Strange 1/22/90
J. E. Strange

TABLE OF CONTENTS

Section	Title	Page
	ABSTRACT.	i
	LIST OF TABLES.	iii
	LIST OF FIGURES	iv
1.0	INTRODUCTION AND CYCLE DESCRIPTION.	1
2.0	TEST PROGRAM SUMMARY.	6
3.0	CORE RELOAD SUMMARY	12
4.0	CORE PERFORMANCE.	15
4.1	INITIAL CRITICALITY	15
4.2	CORE DEPLETION.	15
4.3	REACTIVITY CONTROL.	16
	4.3.1 CONTROL ROD BANK WORTH MEASUREMENTS . . .	16
	4.3.2 BORON WORTH AND ENDPOINT MEASUREMENTS . .	16
4.4	ISOTHERMAL TEMPERATURE COEFFICIENT MEASUREMENTS .	17
4.5	POWER DISTRIBUTION MEASUREMENTS	17
	4.5.1 ASSEMBLY POWER DISTRIBUTIONS.	18
	4.5.2 FQ(Z) SURVEILLANCE.	18
	4.5.3 FDHN SURVEILLANCE	19
	4.5.4 INCORE-EXCORE CALIBRATION	19

LIST OF TABLES

Table	Title	
1.1	SEQUOYAH UNIT 2, CYCLE 5 CORE DESIGN PARAMETERS . .	2
1.2	SEQUOYAH UNIT 2, CYCLE 5 FUEL SPECIFICATIONS. . . .	3
2.1	SEQUOYAH UNIT 2, CYCLE 5 CHRONOLOGY OF STARTUP PHYSICS TESTS	7
2.2	SEQUOYAH UNIT 2, CYCLE 5 SIGNIFICANT EVENTS SUMMARY	8
4.3.1	SEQUOYAH UNIT 2, CYCLE 5 ROD SWAP INTEGRAL BANK WORTHS.	29
4.5.1	SEQUOYAH UNIT 2, CYCLE 5 INCORE FLUX MAP SUMMARY. .	32

LIST OF FIGURES

Figure	Title	
1.1	SEQUOYAH UNIT 2, CYCLE 5 CORE COMPONENT CONFIGURATION	5
2.1	SEQUOYAH UNIT 2, CYCLE 5 MONTHLY REACTOR POWER HISTOGRAM FOR NOVEMBER 1990	10
2.2	SEQUOYAH UNIT 2, CYCLE 5 MONTHLY REACTOR POWER HISTOGRAM FOR DECEMBER 1990	11
3.1	SEQUOYAH UNIT 2, CYCLE 4 FINAL BURNUP DISTRIBUTION.	13
3.2	SEQUOYAH UNIT 2, CYCLE 5 INITIAL CORE LOADING PATTERN	14
4.1.1	SEQUOYAH UNIT 2, CYCLE 5 INVERSE COUNT RATE RATIO DURING ROD WITHDRAWAL FOR N-31.	20
4.1.2	SEQUOYAH UNIT 2, CYCLE 5 INVERSE COUNT RATE RATIO DURING ROD WITHDRAWAL FOR N-32.	21
4.1.3	SEQUOYAH UNIT 2, CYCLE 5 INVERSE COUNT RATE RATIO VERSUS TIME DURING DILUTION N-31.	22
4.1.4	SEQUOYAH UNIT 2, CYCLE 5 INVERSE COUNT RATE RATIO VERSUS TIME DURING DILUTION N-32.	23
4.1.5	SEQUOYAH UNIT 2, CYCLE 5 INVERSE COUNT RATE RATIO VERSUS GALLONS OF DILUTION N-31	24
4.1.6	SEQUOYAH UNIT 2, CYCLE 5 INVERSE COUNT RATE RATIO VERSUS GALLONS OF DILUTION N-32	25
4.1.7	SEQUOYAH UNIT 2, CYCLE 5 INVERSE COUNT RATE RATIO VERSUS BORON CONCENTRATION N-31	26
4.1.8	SEQUOYAH UNIT 2, CYCLE 5 INVERSE COUNT RATE RATIO VERSUS BORON CONCENTRATION N-32	27
4.2.1	SEQUOYAH UNIT 2, CYCLE 5 BORON LETDOWN CURVE. . . .	28
4.3.1	SEQUOYAH UNIT 2, CYCLE 5 INTEGRAL BANK D WORTH. . .	30
4.3.2	SEQUOYAH UNIT 2, CYCLE 5 DIFFERENTIAL BANK D WORTH.	31
4.5.1	SEQUOYAH UNIT 2, CYCLE 5 RELATIVE ASSEMBLY POWERS INC-5-F2-90-1B.	33

LIST OF FIGURES (continued)

4.5.2	SEQUOYAH UNIT 2, CYCLE 5 RELATIVE ASSEMBLY POWERS INC-5-F2-90-2A.	35
4.5.3	SEQUOYAH UNIT 2, CYCLE 5 RELATIVE ASSEMBLY POWERS INC-5-F2-90-11A	37
4.5.4	SEQUOYAH UNIT 2, CYCLE 5 NORMALIZED AVERAGE AXIAL POWER DISTRIBUTION INC-5-F2-90-1B	39
4.5.5	SEQUOYAH UNIT 2, CYCLE 5 NORMALIZED AVERAGE AXIAL POWER DISTRIBUTION INC-5-F2-90-2A	40
4.5.6	SEQUOYAH UNIT 2, CYCLE 5 NORMALIZED AVERAGE AXIAL POWER DISTRIBUTION INC-5-F2-90-11A.	41
4.5.7	SEQUOYAH UNIT 2, CYCLE 5 LIMITING FQ AT EACH AXIAL POINT INC-5-F2-90-1B.	42
4.5.8	SEQUOYAH UNIT 2, CYCLE 5 LIMITING FQ AT EACH AXIAL POINT INC-5-F2-90-2A.	43
4.5.9	SEQUOYAH UNIT 2, CYCLE 5 LIMITING FQ AT EACH AXIAL POINT INC-5-F2-90-11A	44
4.5.10	SEQUOYAH UNIT 2, CYCLE 5 $K(Z)$ - NORMALIZED $FQ(Z)$ AS A FUNCTION OF CORE HEIGHT	45
4.5.11	SEQUOYAH UNIT 2, CYCLE 5 AXIAL FLUX DIFFERENCE LIMITS AS A FUNCTION OF RATED THERMAL POWER	46

1.0 Introduction and Cycle Description

Sequoyah unit 2 was shut down on September 8, 1990, ending its fourth cycle of operation. During the 75 day outage, 80 of the 193 fuel assemblies were replaced with fresh fuel. Ultrasonic fuel inspection identified leaking fuel rods in 4 assemblies scheduled for reinsertion, assemblies S15, S21, S27, and S61. Assemblies S15, S21, and S27 are symmetric counterparts and were discharged. Assembly S61 and three symmetric counterparts were also discharged. In addition, visual inspections identified 18 instances of grid damage, one severe enough to discharge the assembly (assembly S20). Assembly S20 was the fourth symmetric counterpart for S15, S21, and S27. The 80 fresh fuel assemblies consist of 56 3.60 w/o ^{235}U assemblies and 24 4.20 w/o ^{235}U assemblies of the Westinghouse Vantage 5H type. The final core loading pattern is presented in Figure 3.2. Cycle 5 is the first application of the Vantage 5H fuel in unit 2, and includes the following new features; Zircaloy grids, reconstitutable top nozzles, integral fuel burnable absorbers (IFBA), extended burnup capability, and debris filter bottom nozzles.

The purpose of this report is to discuss the cycle 5 startup physics testing program. The startup tests are performed to verify that the core performs as designed. Tables 1.1 and 1.2 contain core design parameters and fuel specifications for cycle 5.

Cycle 5 utilizes 144 fresh burnable absorber rods of the wet annular design in cluster patterns of 4 and 8. In addition, 7104 integral fuel burnable absorbers were used in patterns of 80, 100, and 128 rods per assembly. The neutron sources are located in 2 assemblies each containing 4 source rods. Core locations for the burnable absorbers, neutron sources, and control rods are indicated in Figure 1.1.

Cycle 5 has a projected full power capability of approximately 15,600 MWD/MTU (410 effective full power days, EFPD). The safety analysis for cycle 5 is valid up to a burnup of 16,600 MWD/MTU which includes a power coastdown. Operation of cycle 5 will have the flexibility of being governed by relaxed axial offset control (RAOC).

Table 1.1

Sequoyah Unit 2, Cycle 5 Core Design Parameters

Power Rating	3411 MWT
Heat Generated in Fuel	97.4 %
Coolant Temperatures	
Hot Zero Power	547.0 F
Design Inlet, Hot Full Power	546.7 F
Design Core Average, Hot Full Power	582.2 F
System Pressure	2250 psia
Average Linear Power Density	5.43 kW/ft
Specific Power	38.09 kW/KGU
Power Density	103.79 kW/liter
Hot Channel Factor	
Limiting Heat Flux, FQ	2.32
Nuclear Enthalpy Rise, FDHN	1.55

Table 1.2

Sequoyah Unit 2, Cycle 5 Fuel Specifications

Number of Fuel Assemblies

Region 4	9
Region 5A	24
Region 5B	8
Region 6A	40
Region 6B	32
Region 7A	56
Region 7B	<u>24</u>
Total	193

Region Fuel Loading

Region 4	4.14 MTU
Region 5A	11.08 MTU
Region 5B	3.69 MTU
Region 6A	18.62 MTU
Region 6B	14.91 MTU
Region 7A	25.98 MTU
Region 7B	<u>11.12 MTU</u>
Total	89.54 MTU

Enrichments (w/o U-235)

Region 4	3.50 w/o
Region 5A	3.80 w/o
Region 5B	3.60 w/o
Region 6A	3.40 w/o
Region 6B	3.60 w/o
Region 7A	3.60 w/o
Region 7B	4.20 w/o

Active Fuel Height 144 inches

Lattice Configuration 17 x 17

Lattice Pitch 0.496 inches

Assembly Pitch 8.466 inches

No. of Fuel Rods Per Assembly 264

No. of Instrument Thimbles per Assembly 1

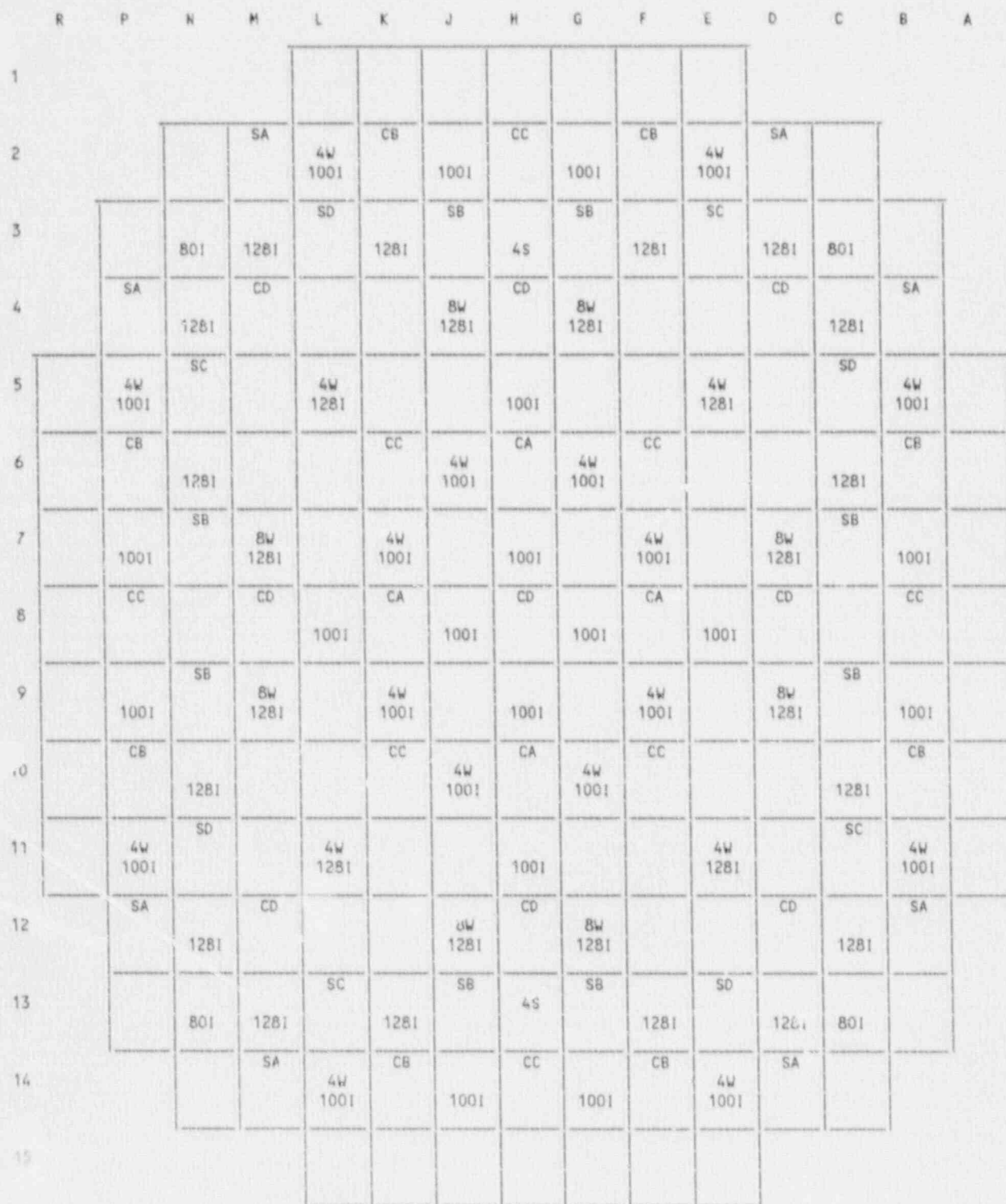
No. of RCC Guide Thimbles Per Assembly 24

No. of Grids Per Assembly 8

Fuel Rod Outside Diameter 0.374 inches

Table 1.2 (Continued)

Clad Thickness	0.0225 inches
Clad Material	Zircaloy-4
Pellet Diameter	0.3225 inches
Wet Annular Burnable Absorbers	144 ($\text{Al}_2\text{O}_3\text{-B}_4\text{C}$)
Integral Fuel Burnable Absorbers	7104 (ZrB_2 coating)



TYPE	TOTAL
CA, CB, CC, CD, SA, SB, SC, SD...(RCCAs).....	53
W....(WABAs).....	144
I....(IFBAs).....	7104
S....(SECONDARY SOURCE RODLETS).....	8

FIGURE 1.1 SEQUOYAH UNIT 2 CYCLE 5 CORE COMPONENT CONFIGURATION

2.0 Test Program Summary

This report covers the period from September 21, 1990 through December 31, 1990. Significant milestones for this period are summarized as follows:

Start of Core Unload	September 21, 1990
End of Core Reload	October 11, 1990
Initial Criticality	November 12, 1990
Completion of Zero Power Physics Testing	November 21, 1990
Initial Power Generation	November 22, 1990
Power Escalation to 30-percent Power	November 22, 1990
Power Escalation to 70-percent Power	November 30, 1990
Power Escalation to 100-percent Power	December 6, 1990
Achieved Core Burnup of 32 EFPD	December 31, 1990

Table 2.1 summarizes the startup physics tests that were performed during cycle 5 startup. Reactor power histograms for November 1990 and December 1990 are shown in Figures 2.1 and 2.2, respectively, with significant events summarized in Table 2.2.

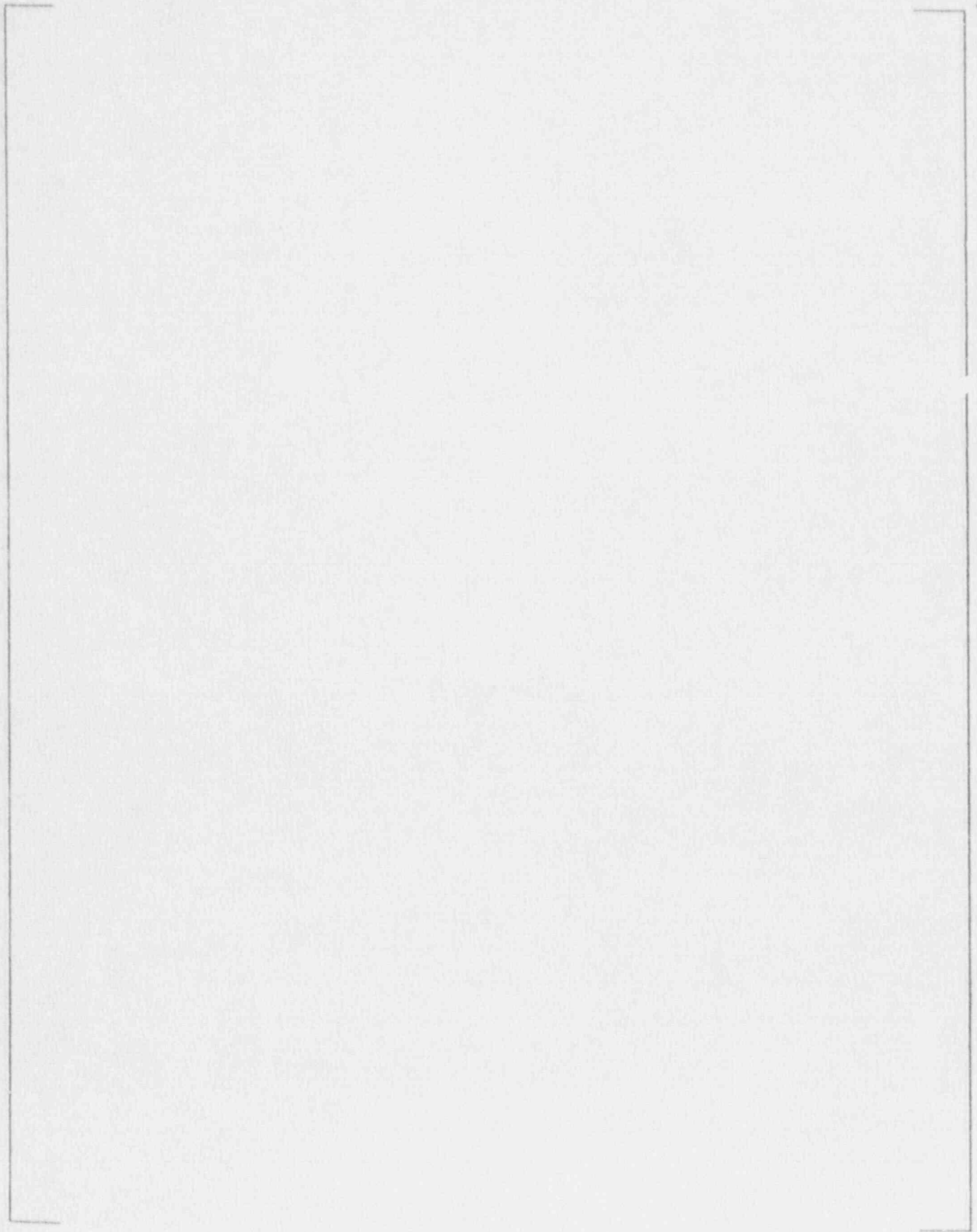


FIGURE 3.2 SEQUOYAH UNIT 2 CYCLE 5 INITIAL CORE LOADING PATTERN

4.0 Core Performance

The operational power capabilities of Sequoyah Nuclear Plant are governed by limits imposed by the safety analysis, as presented in the Sequoyah Updated Final Safety Analysis Report (UFSAR). Various core parameters were measured during the restart physics testing to ensure the conservatism of assumptions made in the safety analysis and to verify the core performed as designed. The following sections discuss the results of the core physics tests.

4.1 Initial Criticality

Initial criticality was achieved on November 12, 1990 at 1730 EST. The reactor coolant system temperature and pressure were about 547 F and 2235 psig, respectively. The soluble boron concentration was 1513 ppm, and all rod control banks were fully withdrawn with the exception of control bank D, which was at 200.5 steps. The corrected critical boron concentration for control bank D at 200 steps was 1513 ppm. The acceptance criterion for critical boron concentration with control bank D at 200 steps was [] \pm 130 ppm.

a,c

The approach to criticality proceeded in a safe and judicious manner. Starting with the shutdown banks withdrawn and 1751 ppm and the reactor coolant at about 547 F and 2235 psig, control rod withdrawal commenced. During rod withdrawal, inverse count rate ratio data was recorded and plotted for source range detectors N-31 and N-32 (Figures 4.1.1 through 4.1.2). When control banks A, B, and C were fully withdrawn and control bank D was positioned at about 200 steps, boron dilution was initiated. Again inverse count rate ratio plots were recorded (Figures 4.1.3 through 4.1.8). The reactor coolant was diluted until criticality was achieved.

In addition to bringing the reactor critical for the first time, the initial criticality procedure accomplished several other objectives. The neutron flux level at which nuclear heating first occurred was determined, thus establishing a range below nuclear heating at which all zero power physics measurements were performed. The calibration of the reactivity computer was verified by comparing its output to several positive and negative reactor periods.

4.2 Core Depletion

The primary coolant critical boron concentration is monitored for the purposes of following core reactivity and identifying any anomalous reactivity behavior. If necessary, the measured

critical boron concentration is adjusted to nominal 100-percent operation conditions taking into consideration control rod position, xenon and samarium concentrations, moderator temperature, and power level. Figure 4.2.1 shows the design boron letdown curve and the measured critical boron concentration versus burnup to about 32 EFPD in cycle 5.

4.3 Reactivity Control

Excess reactivity is controlled by neutron absorbing control rods, boric acid dissolved in the reactor coolant and burnable absorbers. Both the control rod position and the boron concentration may be adjusted separately or in conjunction with one another to compensate for various reactivity changes and to maintain the required shutdown margin. Rod bank and boron reactivity worths are measured at hot zero power (H2P) for comparison with design predictions.

4.3.1 Control Rod Bank Worth Measurements

Control rod bank worth measurements for cycle 5 were determined using the Westinghouse rod swap procedure. This replaces the standard boration/dilution method for determining the integral and differential worths of each control rod bank.

The rod swap procedure starts with the measurement of the reference bank worth using the boron exchange technique. After establishing an equilibrium condition with the reference bank inserted, each remaining rod bank is inserted and the reactivity change is compensated by withdrawing the reference bank. For the cycle 5 loading pattern, control bank D was used as the reference bank. The measured integral worth of control bank D was 1102.7 pcm, which met the acceptance criteria of [] ± 162 pcm. Figures 4.3.1 and 4.3.2 provide plots of the integral and differential worth of control bank D. Table 4.3.1 shows a comparison of measured and predicted rod worths based on the rod swap.

a,c

4.3.2 Boron Worth and Endpoint Measurements

Reactor coolant system boron measurements were made during zero power physics testing to determine differential boron worth and concentration endpoints for the ARO configuration. The differential boron worth measured over the range of control bank D at H2P was -7.95 pcm/ppm. The measured differential boron worth was within the review criteria of [] ± 1.17 pcm/ppm. The boron endpoint was established for the ARO configuration. The boron endpoint value includes corrections to the measured data to account for differences between the critical

a,c

configuration and the endpoint configuration. The ARO boron endpoint was calculated to be 1527 ppm, well within the review criteria of [] ± 50 ppm.

a,c

4.4 Isothermal Temperature Coefficient Measurements

The isothermal temperature coefficient (ITC) was measured during zero power physics testing to verify a negative moderator temperature coefficient (MTC) as required by Technical Specifications. The ITC is defined as the change in core reactivity per unit change in moderator, clad, and fuel temperatures. From the measured ITC, a value for the MTC is obtained from the relationship:

$$\text{MTC} = \text{ITC} - \text{Doppler Coefficient}$$

The predicted hot zero power beginning of cycle Doppler coefficient was [] pcm/F.

a,c

This measurement was performed by heating up and cooling down the primary system by regulating steam dump to the atmosphere or the condenser over the range of 543 to 546 F. During the heatup and cooldown, an X-Y recorder was utilized to plot the change in reactivity with respect to the changes in the primary system temperature. The slope of this curve of T_{avg} versus reactivity is the ITC.

Measurements of the ITC were taken for D bank at 213 steps. The ITC measured during heatup and cooldown were -2.98 and -2.66 pcm/F respectively, with an average of -2.82 pcm/F at a T_{avg} of 544.8 F. When corrected to a temperature of 547 F and ARO, the ITC was found to be -2.90 pcm/F which is within the acceptance criteria of [] ± 2 pcm/F. When conservatively corrected to a T_{avg} of 541 F, the corrected ITC is -2.38 pcm/F. The corresponding conservative MTC was -0.48 pcm/F which is within the acceptance criteria of < 0 pcm/F.

a,c

4.5 Power Distribution Measurements

Analysis of core power distribution data during startup testing is necessary to verify proper core loading, design calculations, compliance with Technical Specifications, and the relationship between incore power distributions and excore detector responses. Three-dimensional core power distributions are determined from moveable detector flux trace measurements using the INCORE computer code.

Table 4.5.1 summarizes representative INCORE flux maps for the startup of unit 2, cycle 5. This table includes the core

conditions at the time of the measurement and INCORE results for the maximum heat flux hot channel factor (excluding uncertainties) $FQN(z)$, the maximum nuclear enthalpy rise hot channel factor $FDHN$, incore quadrant power tilt ratios (QPTR), and axial offsets. Note that the maximum peaking factors identified in Table 4.5.1 are useful from a core design standpoint, but are not necessarily the most limiting according to Technical Specifications since they do not indicate reduced margins associated with the $W(z)$ and $K(z)$ functions or uncertainty tolerances.

4.5.1 Assembly Power Distributions

Power distribution measurements were made during startup testing at 30-percent power, 70-percent power, and 100-percent power. Relative assembly power is analyzed with respect to the difference between designed and measured values. Figures 4.5.1 through 4.5.3 provide an assemblywise relative power distribution for all the flux maps described in Table 4.5.1. Also included in these figures are comparisons between measured and designed assembly powers including the RMS difference, the RMS percent difference, the RMS difference for assemblies above 1.0 relative power, the out-in power tilt (power in the outer two rings of assemblies vs. the power in the center), the incore quadrant power tilt and the maximum percent difference between symmetric assemblies.

When the 30-percent power flux map was recorded and compared to predictions, all review criteria were met. Flux maps were also recorded at 70-percent and 100-percent power.

Figures 4.5.4 through 4.5.6 illustrate the normalized core average axial power distributions for each flux map.

4.5.2 $Fq(z)$ Surveillance

The Technical Specification limit for $Fq(z)$ at full power is 2.32. $Fq(z)$ surveillance involves the use of the parameter $K(z)$. $K(z)$ is $Fq(z)$ normalized to the maximum value allowed at any core height. The parameter $K(z)$ is given in Figure 4.5.10 for unit 2, cycle 5 operation. Operation of cycle 5 has had the added flexibility of Relaxed Axial Offset Control (RAOC). Figure 4.5.11 represents the acceptable RAOC delta-I operation limits used in cycle 5. The Technical Specification surveillance requirement on $Fq(z)$ incorporates potential changes from the equilibrium power distribution by using a transient function $W(z)$. $W(z)$ accounts for the effects of normal operational transients and is determined from calculated power control maneuvers over the full range of burnup, power, and axial flux difference conditions. The $Fq(z)$ limit of 2.32 is multiplied by $K(z)/W(z)$ and then compared with the measured $Fq(z)$ values.

Figures 4.5.7 through 4.5.9 illustrate the $F_q(z)$ limit and limiting value at each axial point for each flux map.

4.5.3 FDHN Surveillance

FDHN surveillance is accomplished by comparison of the measured FDHN to the FDHN limit defined by plant Technical Specifications. The Technical Specification limit for FDHN at full power is 1.55. The measured value of FDHN obtained in each flux map was verified to be within Technical Specification limits.

4.5.4 Incore-Excore Calibration

Calibration of the nuclear instrumentation system (NIS), comprised of six moveable incore detectors and eight stationary excore detectors, is required for each core reload. For this cycle, calibrations were performed for startup, at 30-percent power, and at 70-percent power. The calibration at 30-percent was a single point alignment. Calibration checks were performed on the Intermediate Range channels at 50-percent and 100-percent power. A calibration was required at 50-percent power.

To obtain the data required to calibrate the NIS excore power range detectors at power, an axial xenon oscillation is induced in the core by inserting control bank D. After about 5 hours, control bank D is withdrawn to its starting position and the xenon oscillation is allowed to swing delta-I without any adjustments in bank D position.

Full-core flux maps are taken along with associated NIS and calorimetric data prior to the oscillation and at the peak of the delta-I swing. From this data the power range channels N-41 through N-44 were calibrated.

ICRR During Rod Withdrawal For N-31

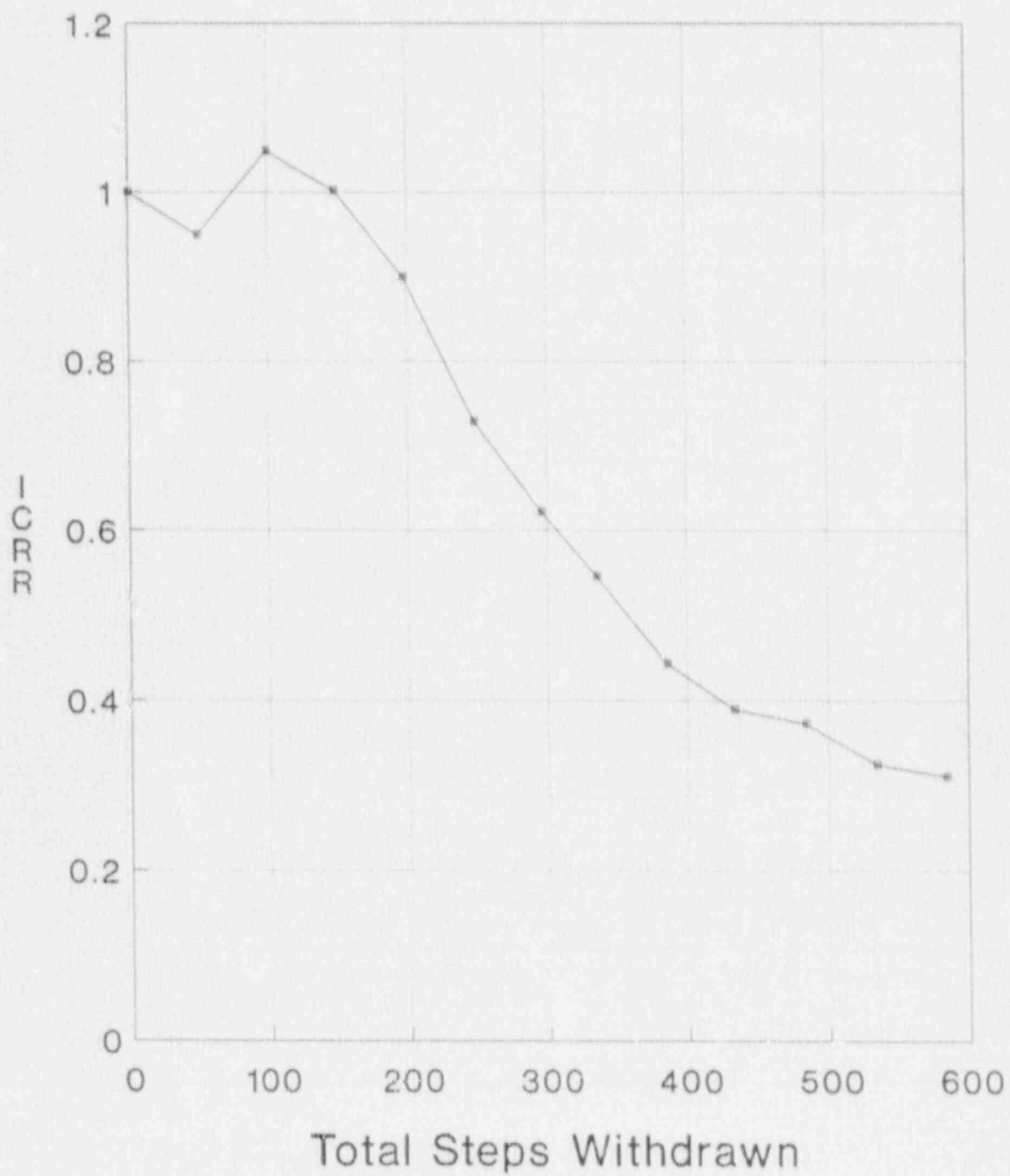


Figure 4.1.1

ICRR During Rod Withdrawal For N-32

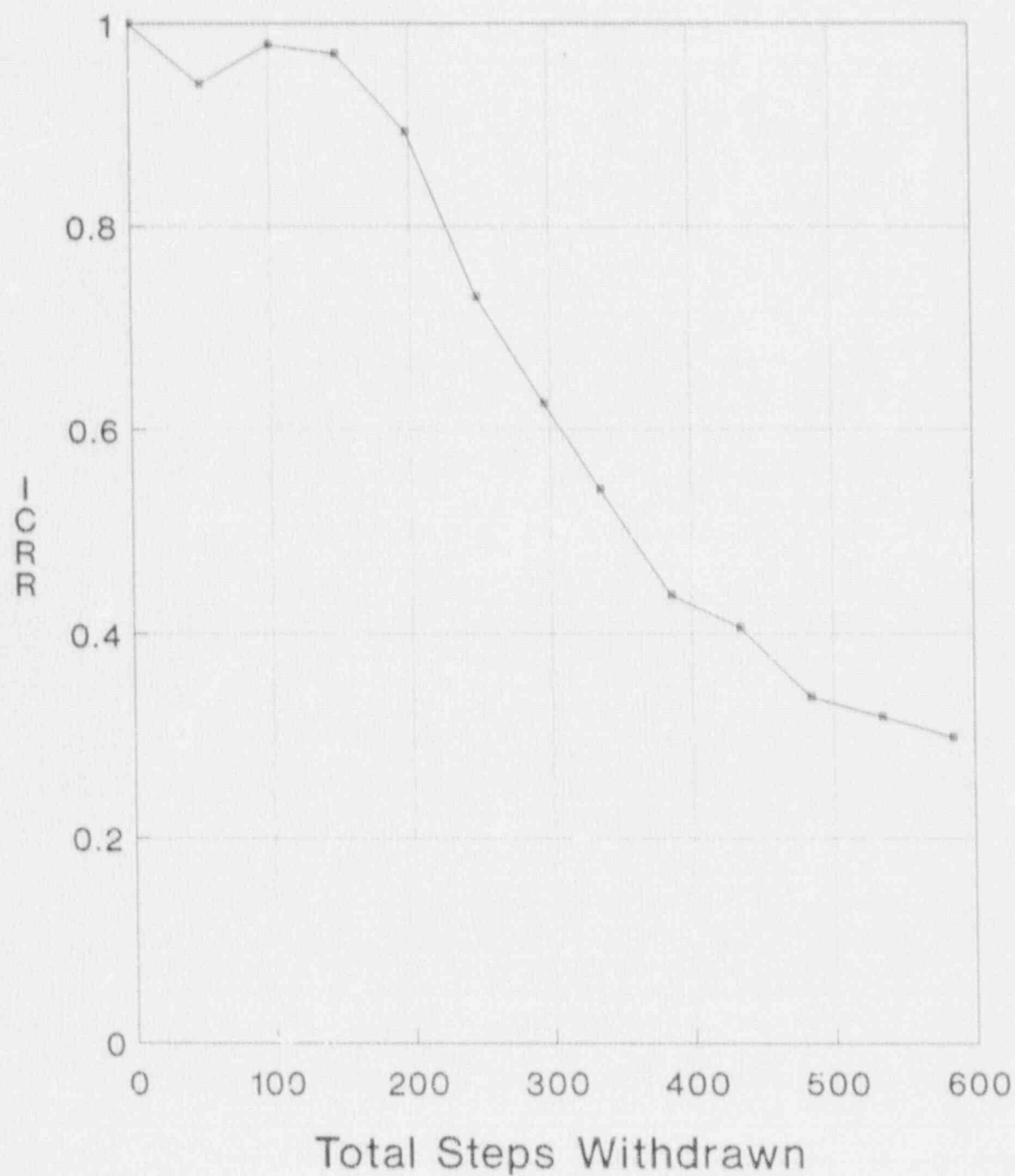


Figure 4.1.2

ICRR Versus Time During Dilution N-31

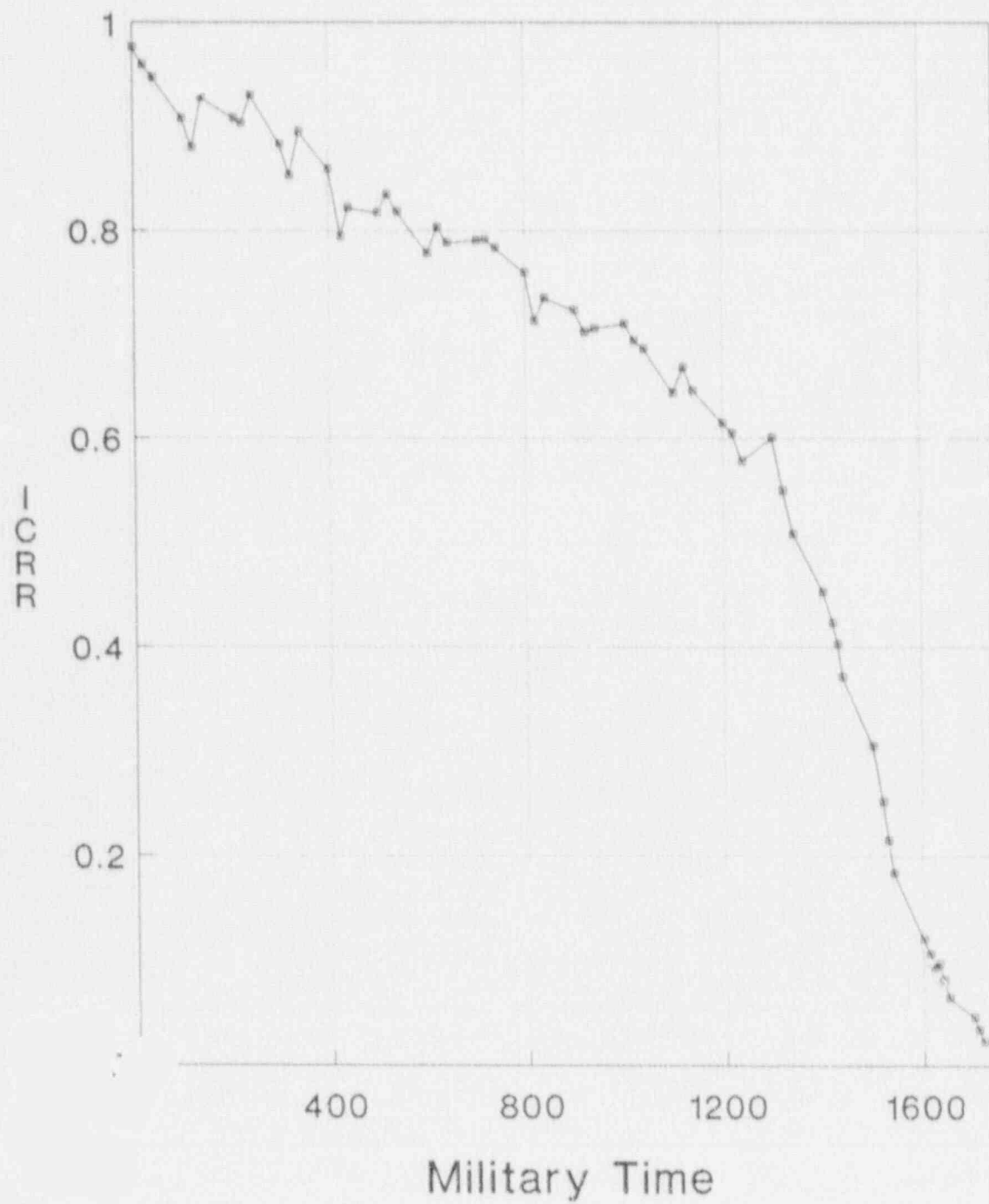


Figure 4.1.3

ICRR Versus Time During Dilution N-32

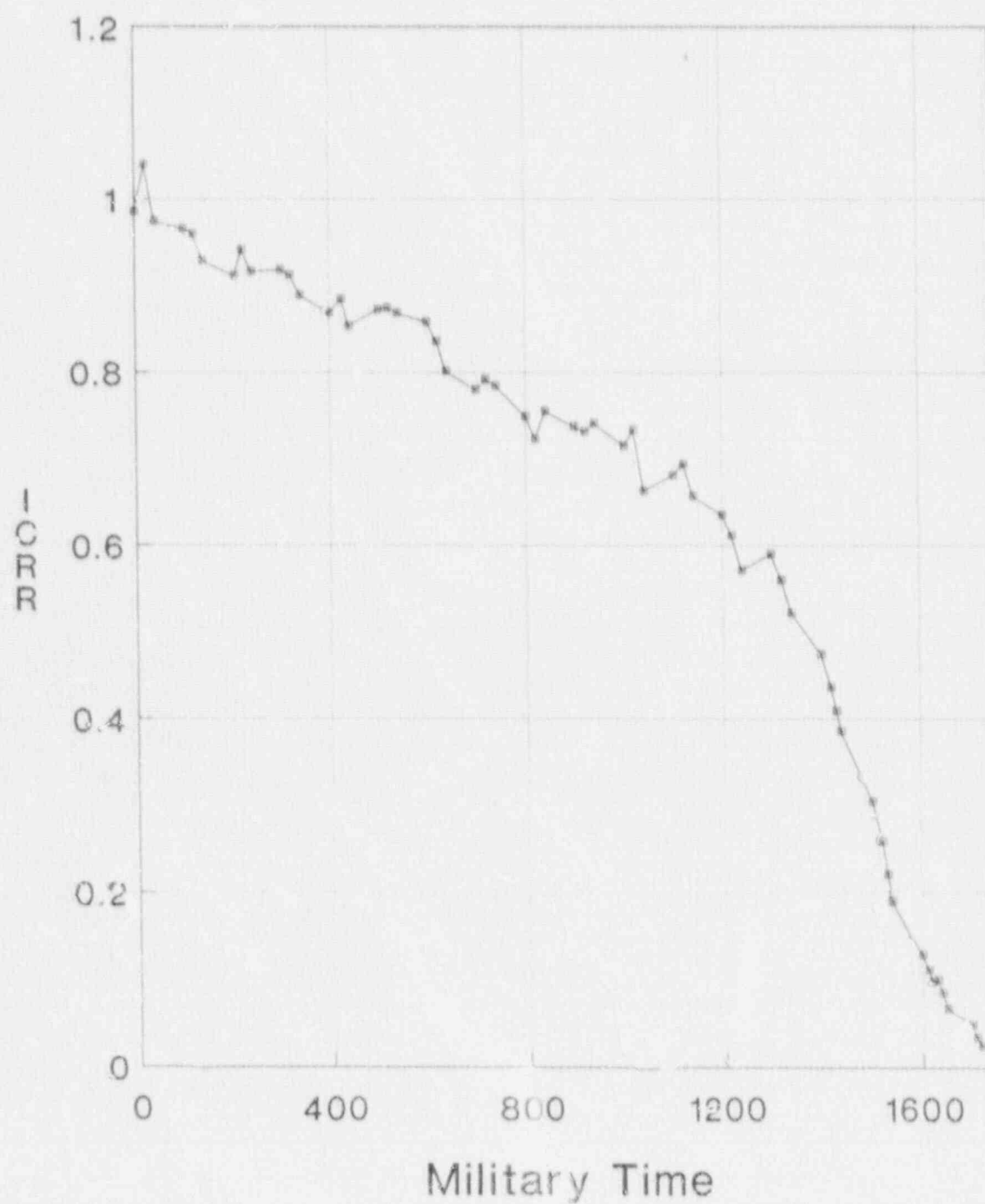


Figure 4.1.4

ICRR Versus Gallons of Dilution N-31

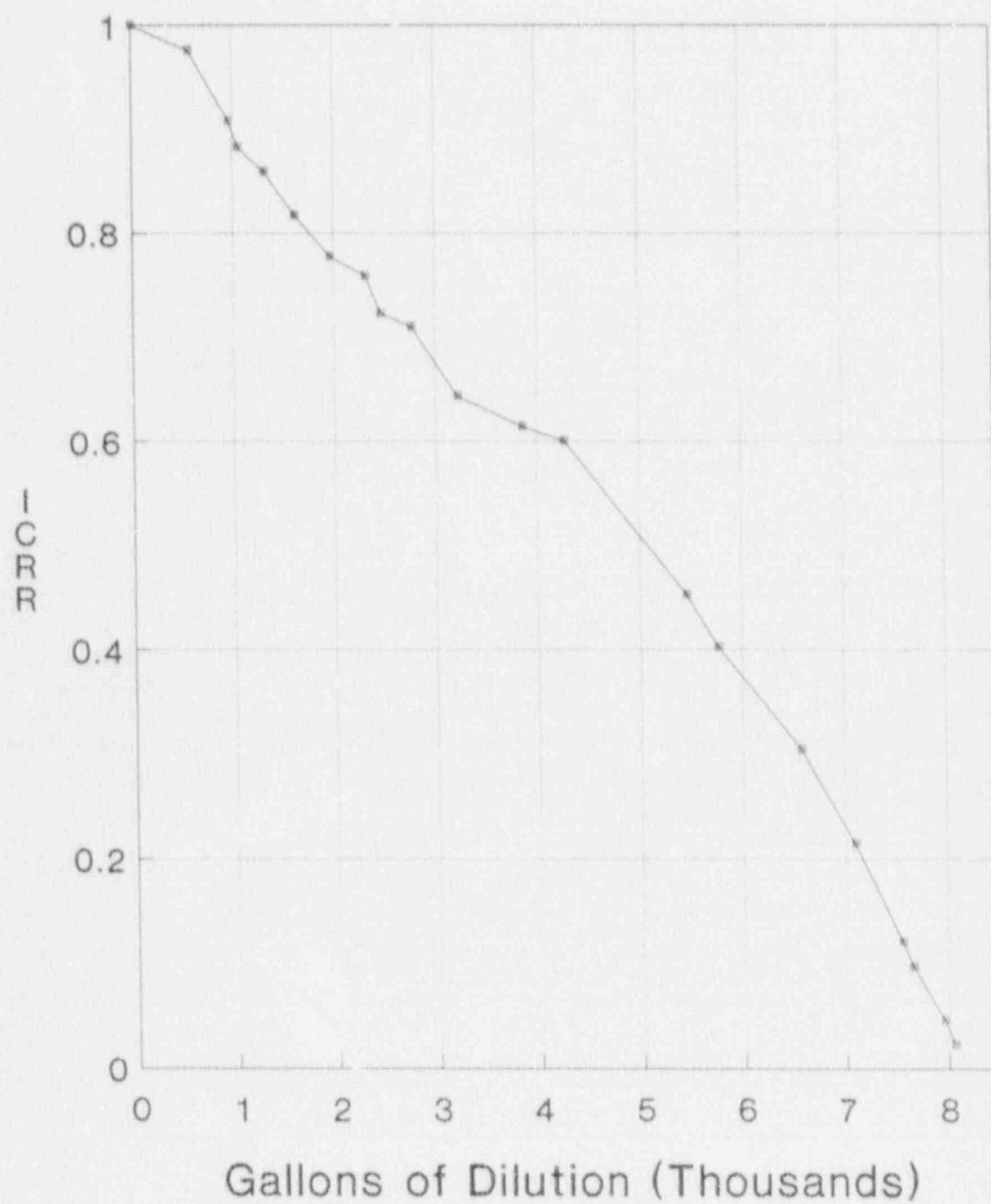


Figure 4.1.6

ICRR Versus Gallons of Dilution N-32

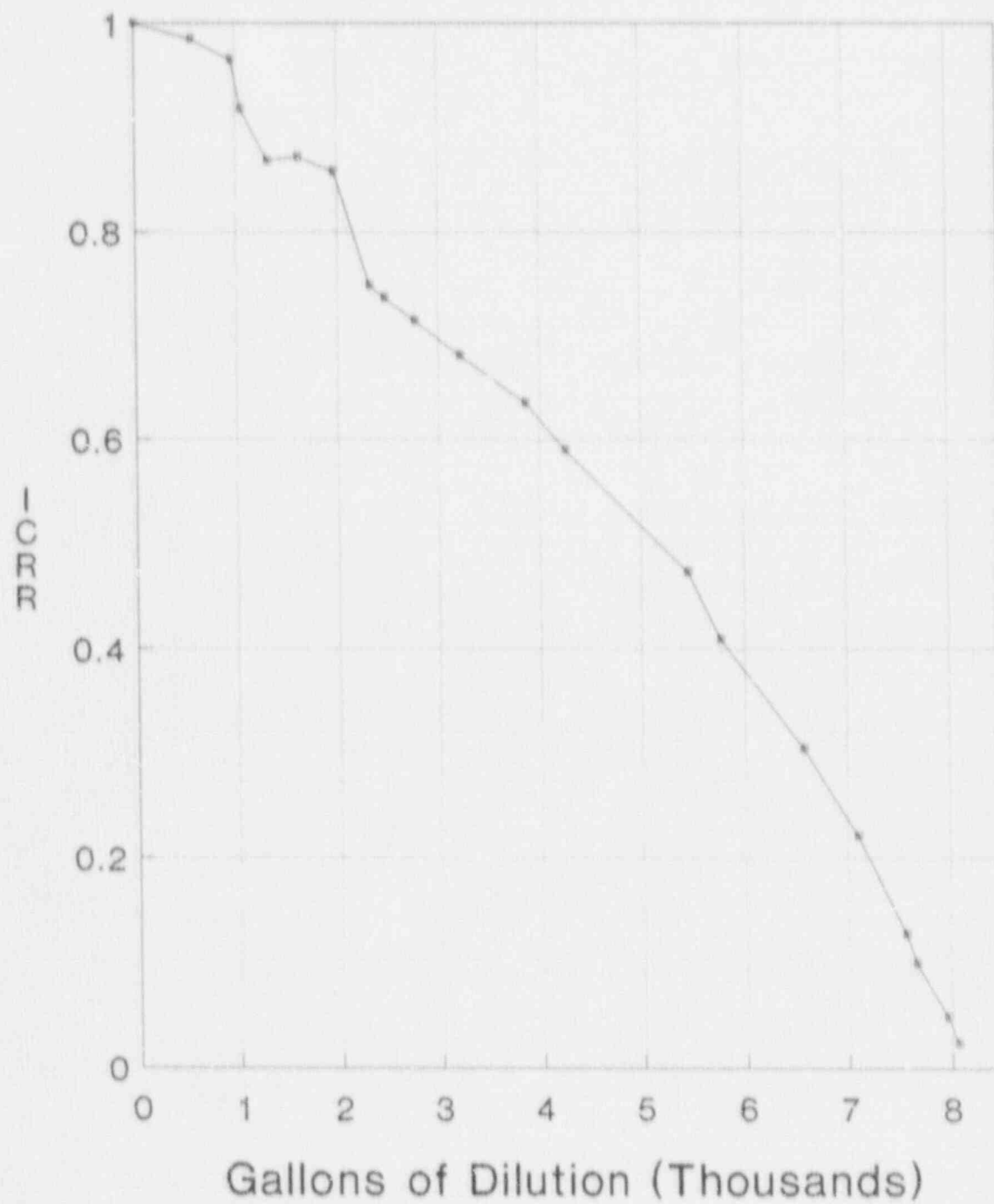


Figure 4.1.6

ICRR Versus Boron Concentration N-31

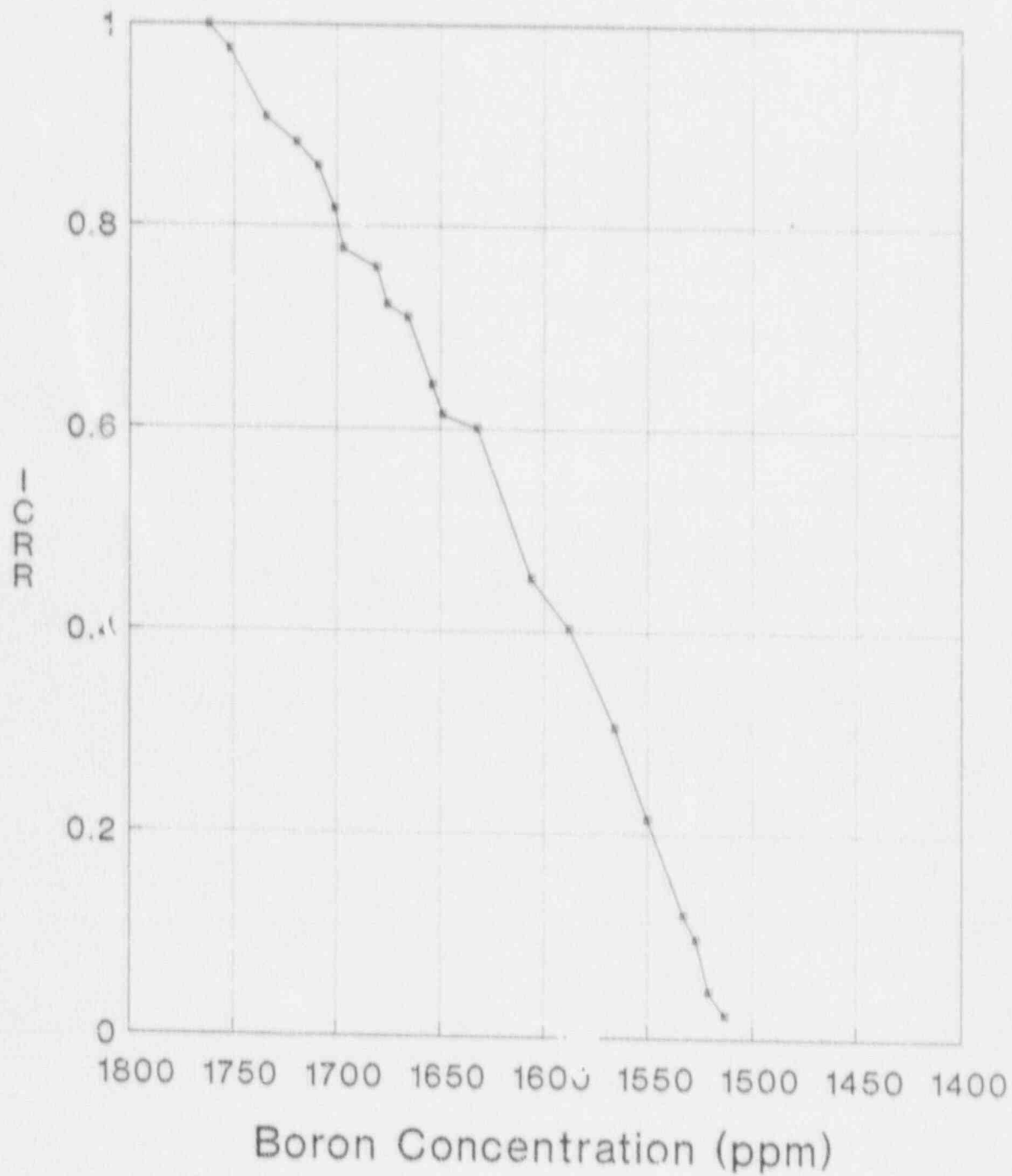


Figure 4.1.7

ICRR Versus Boron Concentration N-32

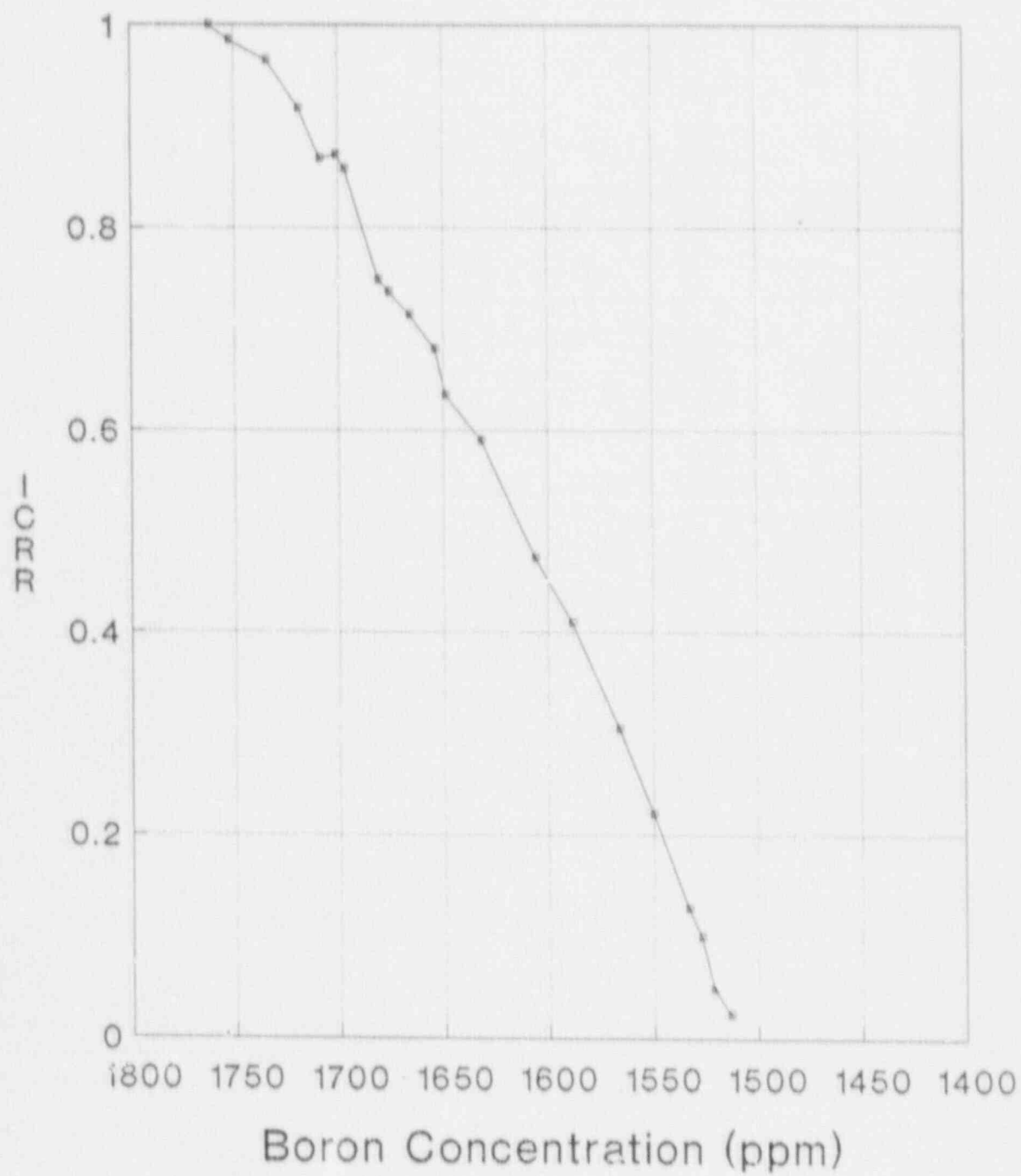


Figure 4.1.8

Figure 4.2.1

Westinghouse Proprietary Class 2

a, c

BORON CONCENTRATION (PPM) AS A FUNCTION OF BURNUP (MWD/MTU)

Table 4.3.1

Sequoyah Unit 2, Cycle 5 Rod Swap Integral Bank Worths

<u>Bank</u>	<u>Measured Worth (pcm)</u>	[] a,c	
D**	1102.7		
C	794.4		
B	697.3		
A	277.6		
SD	382.4		
SC	382.8		
SB	809.9		
SA	405.2		

* Calculated using $([\text{Measured} - \text{Predicted}]/\text{Predicted}) * 100$

** Bank worth measured by boron exchange method

SQN 2 Cycle 5 Integral Bank D Worth
BOL, HZP, NO XE

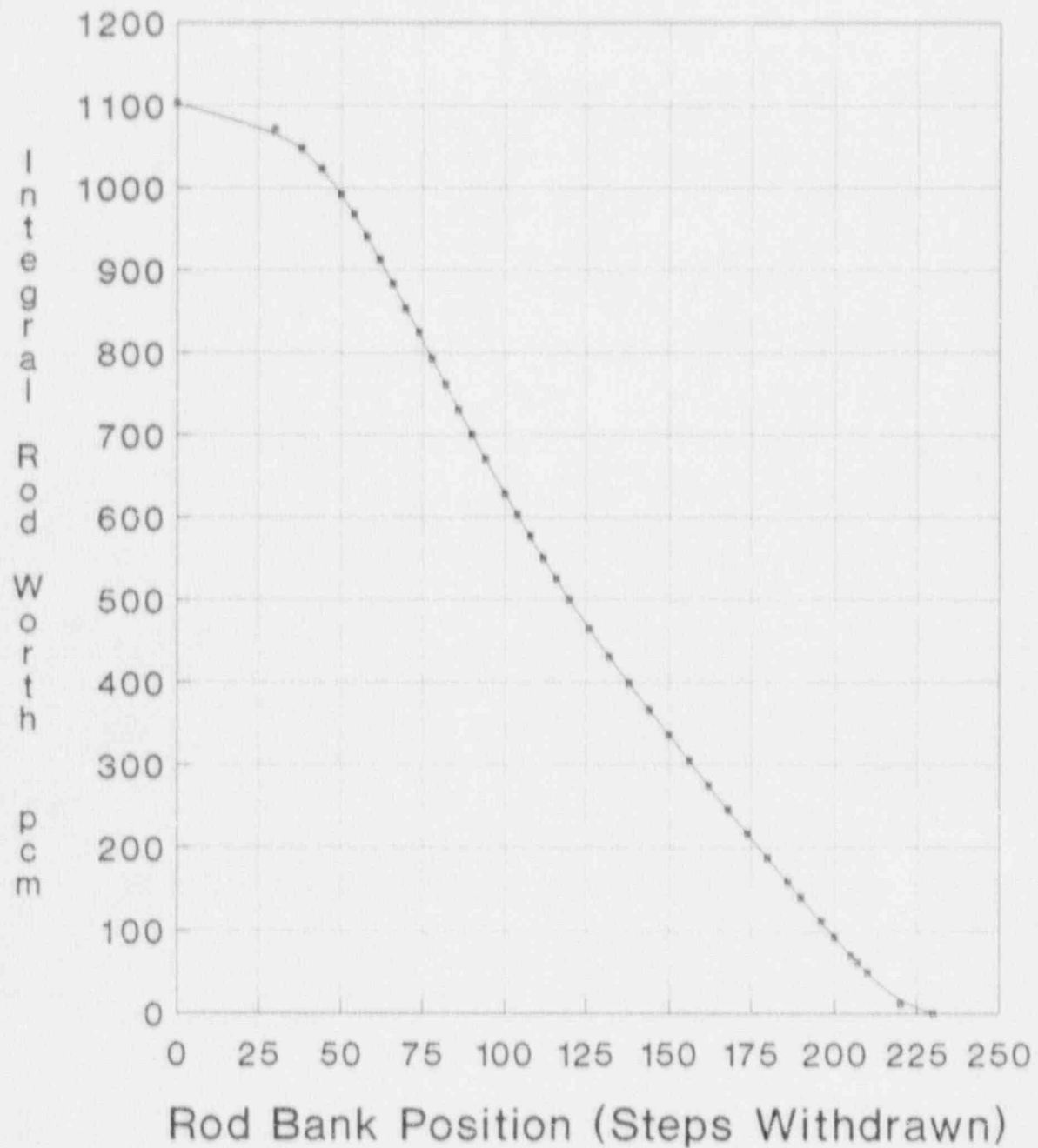


Figure 4.3.1

SQN 2 Cycle 5 Differential Bank D Worth
BOL, HZP, NO XE

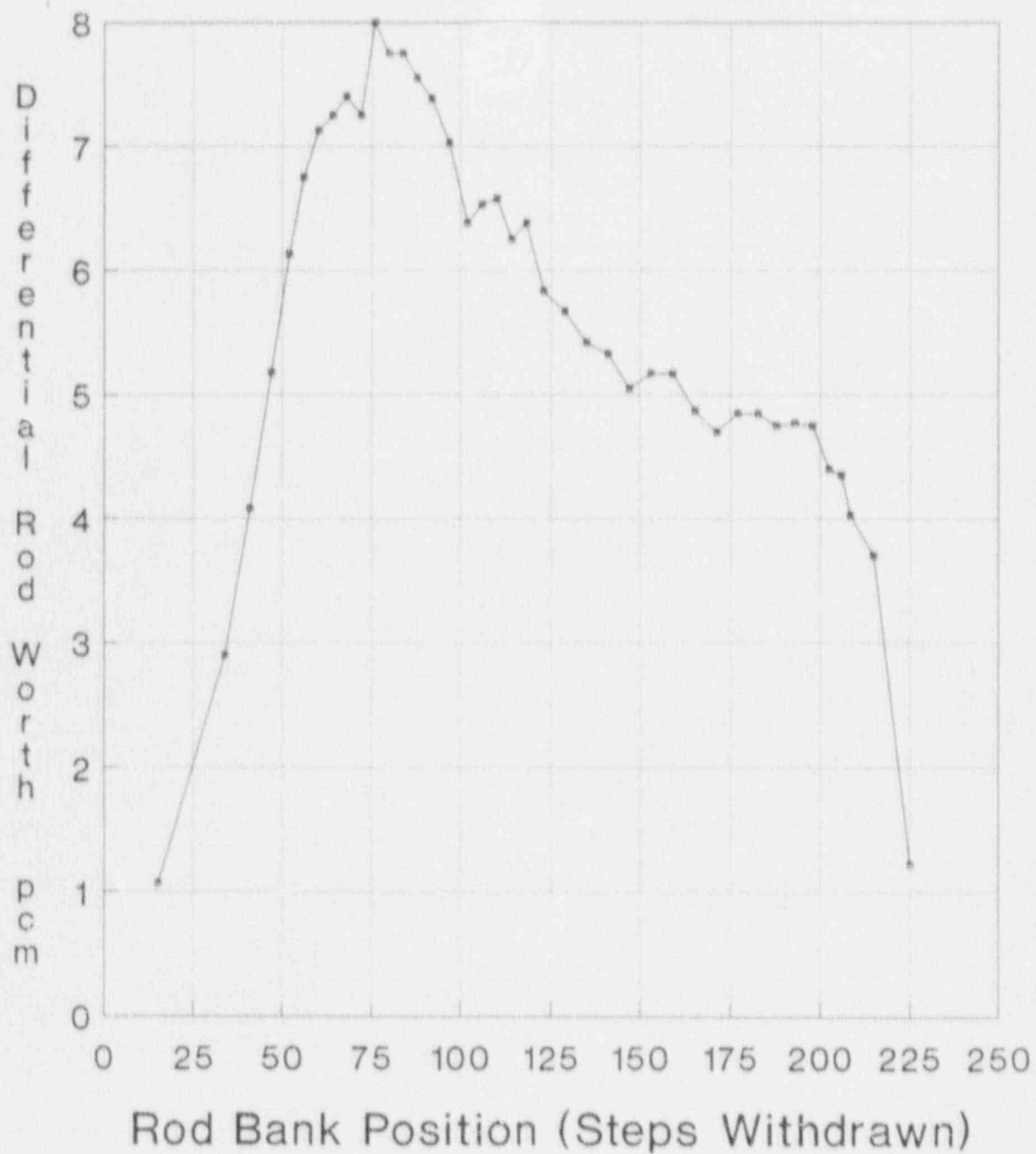


Figure 4.3.2

Westinghouse Proprietary Class 2

TABLE 4.5.1 SEQUOYAH UNIT 2 CYCLE 5 INCORE FLUX MAP SUMMARY

DATE	INC-5-FZ-	BANK D	POWER LEVEL	BURNUP MWD/MTU	MAX FQW(Z)	RADIAL LOCATION	AXIAL POINT	MAX FDHN	RADIAL LOCATION	QPTR*				AXIAL OFFSET	a, c
						a, c			a, c	N41	N42	N43	N44		
11/27/90	90-1B	167.0	27%	22		N 6NM	30		N 6NM	1.0101	0.9797	1.0040	1.0062		
12/ 2/90	90-2A	210.0	71%	135		N 6NM	31		N 6NM	1.0069	0.9853	1.0026	1.0052		
12/ 8/90	90-11A	219.5	100%	307		N 6NM	40		N 6NM	1.0039	0.9899	1.0006	1.0056		

* Relative Locations of Excore Detectors:

N41	N43
N44	N42

B, C

FIGURE 4.5.1 SEQUOYAH UNIT 2 CYCLE 5 RELATIVE ASSEMBLY POWERS
INC-5-F2-90-1B

POWER DISTRIBUTION PARAMETERS

INC-5-F2-90-1B

RMS DIFF = 0.03109 RMS % DIFF = 3.2423

RMS DIFF FOR ASSY > 1.0 RPD = 0.03148

POWER OUT (EXPECTED) = 0.8533
 POWER OUT (MEASURED) = 0.8486
 POWER IN (EXPECTED) = 1.1131
 POWER IN (MEASURED) = 1.1166

MEASURED QUADRANT POWER TILTS
 1.0100 1.0040
 1.0062 0.9797

EXPECTED QUADRANT POWER TILTS
 1.0000 1.0000
 1.0000 1.0000

SYMMETRIC ASSEMBLY % DIFFERENCES

0.00	1.47	2.81	6.54	5.47	5.03	2.68	2.63
1.47	3.78	5.82	5.53	5.84	4.74	4.10	4.63
2.81	2.83	3.73	1.80	6.32	5.65	12.88	11.51
6.54	4.54	0.80	2.74	4.91	6.17	14.32	13.77
5.47	4.43	1.47	1.68	5.00	8.51	13.71	
5.03	4.06	4.61	3.36	8.66	3.47	7.05	
2.68	4.16	3.71	4.00	6.92	5.77		
2.63	6.31	4.10	3.87				

FIGURE 4.5.1 (cont.)

a, c

FIGURE 4.5.2 SEQUOYAH UNIT 2 CYCLE 5 RELATIVE ASSEMBLY POWERS
INC-5-F2-90-2A

POWER DISTRIBUTION PARAMETERS

INC-5-F2-90-2A

RMS DIFF = 0.02299 RMS % DIFF = 2.4431

RMS DIFF FOR ASSY > 1.0 RPD = 0.02266

POWER OUT (EXPECTED) = 0.8429
 POWER OUT (MEASURED) = 0.8354
 POWER IN (EXPECTED) = 1.1211
 POWER IN (MEASURED) = 1.1268

MEASURED QUADRANT POWER TILTS
 1.0068 1.0026
 1.0052 0.9854

EXPECTED QUADRANT POWER TILTS
 1.0000 1.0000
 1.0000 1.0000

SYMMETRIC ASSEMBLY % DIFFERENCES

0.00	2.42	2.14	5.21	5.60	3.98	3.02	2.49
2.42	4.95	5.19	4.52	5.06	3.75	3.22	2.00
2.14	2.87	3.20	1.90	4.31	4.06	9.75	8.51
5.21	2.85	0.54	2.42	3.14	4.05	11.95	11.45
5.60	4.70	1.05	2.57	2.70	6.07	10.30	
3.98	3.49	3.83	2.97	2.94	1.98	5.91	
3.02	3.34	3.13	2.95	6.57	4.10		
2.49	4.43	3.39	2.93				

FIGURE 4.5.2 (cont.)

a,c

FIGURE 4.5.3 SEQUOYAH UNIT 2 CYCLE 5 RELATIVE ASSEMBLY POWERS
INC-5-F2-90-11A

POWER DISTRIBUTION PARAMETERS

INC-5-F2-90-11A

RMS DIFF = 0.01818 RMS % DIFF = 1.9246

RMS DIFF FOR ASSY > 1.0 RPD = 0.01804

POWER OUT (EXPECTED) = 0.8418
 POWER OUT (MEASURED) = 0.8338
 POWER IN (EXPECTED) = 1.1219
 POWER IN (MEASURED) = 1.1281

MEASURED QUADRANT POWER TILTS
 1.0039 1.0005
 1.0057 0.9899

EXPECTED QUADRANT POWER TILTS
 1.0000 1.0000
 1.0000 1.0000

SYMMETRIC ASSEMBLY % DIFFERENCES

0.00	0.87	2.38	5.02	4.43	4.11	3.22	2.92
0.87	3.34	4.37	3.93	3.76	3.42	2.06	0.68
2.38	1.85	2.48	1.54	3.05	3.52	7.38	6.04
5.02	2.55	1.07	1.54	2.34	3.55	9.26	8.72
4.43	4.12	2.29	1.42	1.49	4.21	7.84	
4.11	3.88	3.78	1.22	2.51	3.43	4.31	
3.22	3.26	3.86	1.30	4.47	3.26		
2.92	3.97	3.97	0.92				

FIGURE 4.5.3 (cont.)

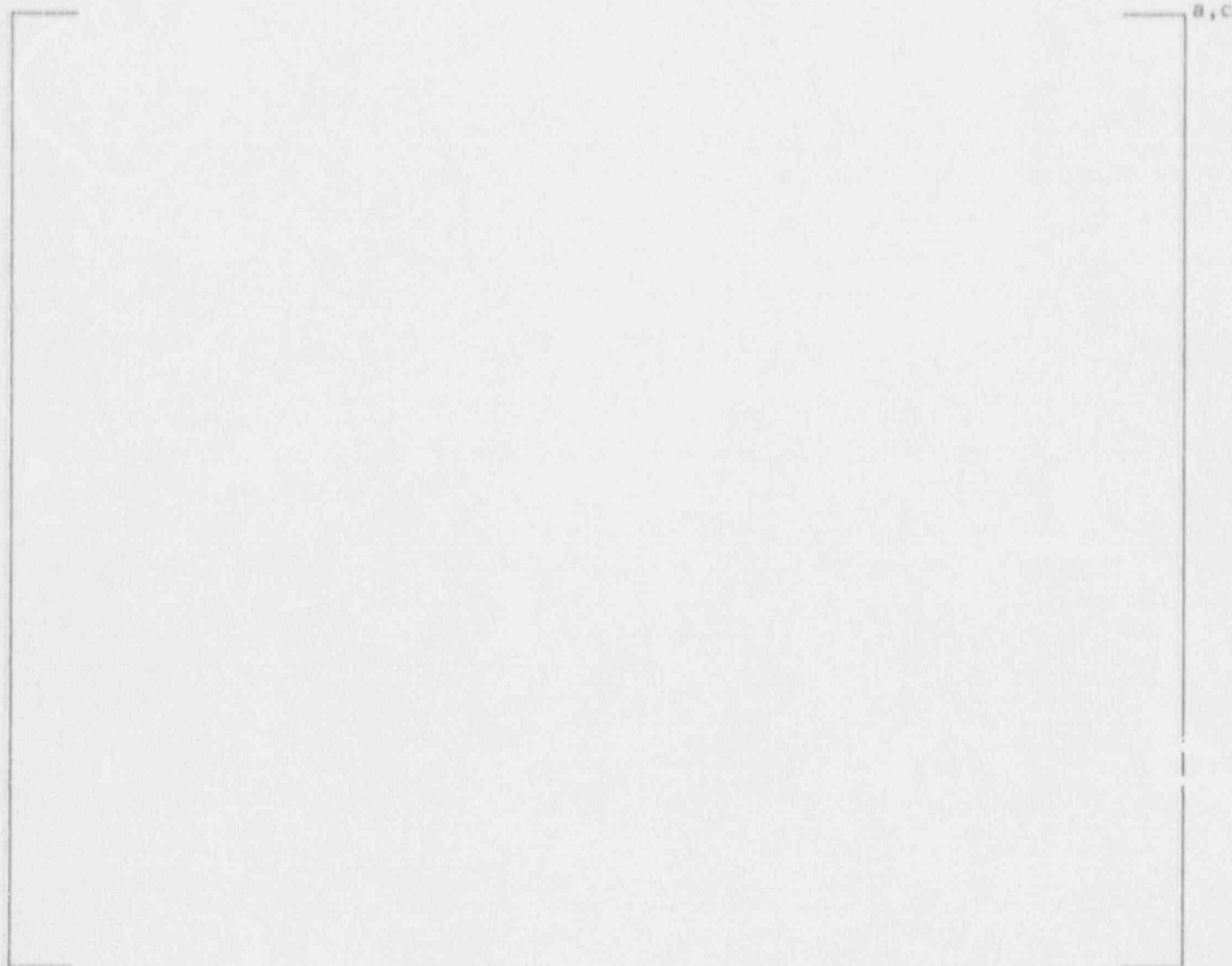


FIGURE 4.5.4 SEQUOIAH UNIT 2 CYCLE 5 NORMALIZED AVERAGE
AXIAL POWER DISTRIBUTION
INC-5-F2-90-1B

a, c

FIGURE 4.5.5 SEQUOYAH UNIT 2 CYCLE 5 NORMALIZED AVERAGE
AXIAL POWER DISTRIBUTION
INC-5-F2-90-2A

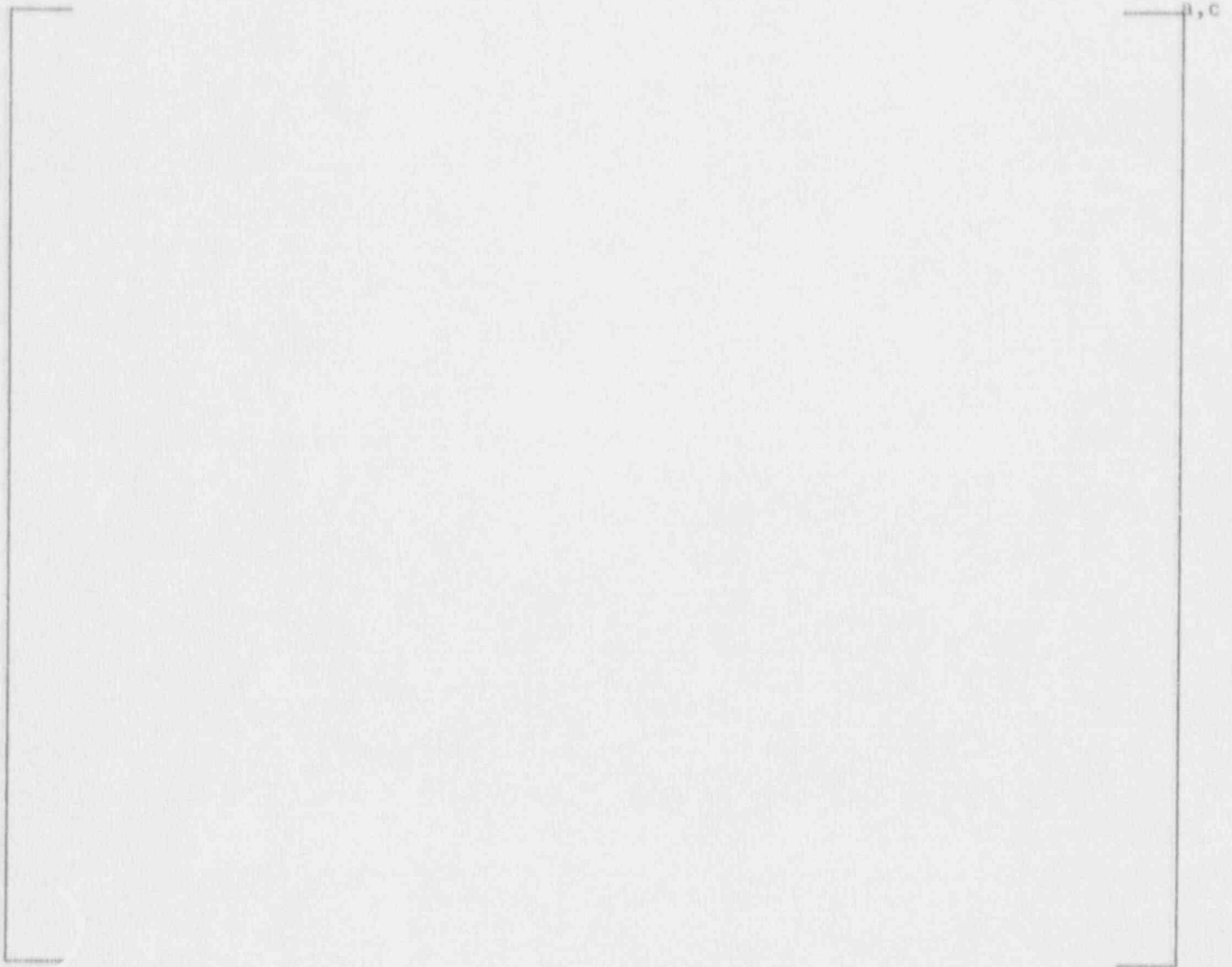


FIGURE 4.5.6 SEQUOYAH UNIT 2 CYCLE 5 NORMALIZED AVERAGE
AXIAL POWER DISTRIBUTION
INC-5-F2-90-11A



FIGURE 4.5.7 SEQUOYAH UNIT 2 CYCLE 5 LIMITING FQ
AT EACH AXIAL POINT
INC-5-F2-90-1B

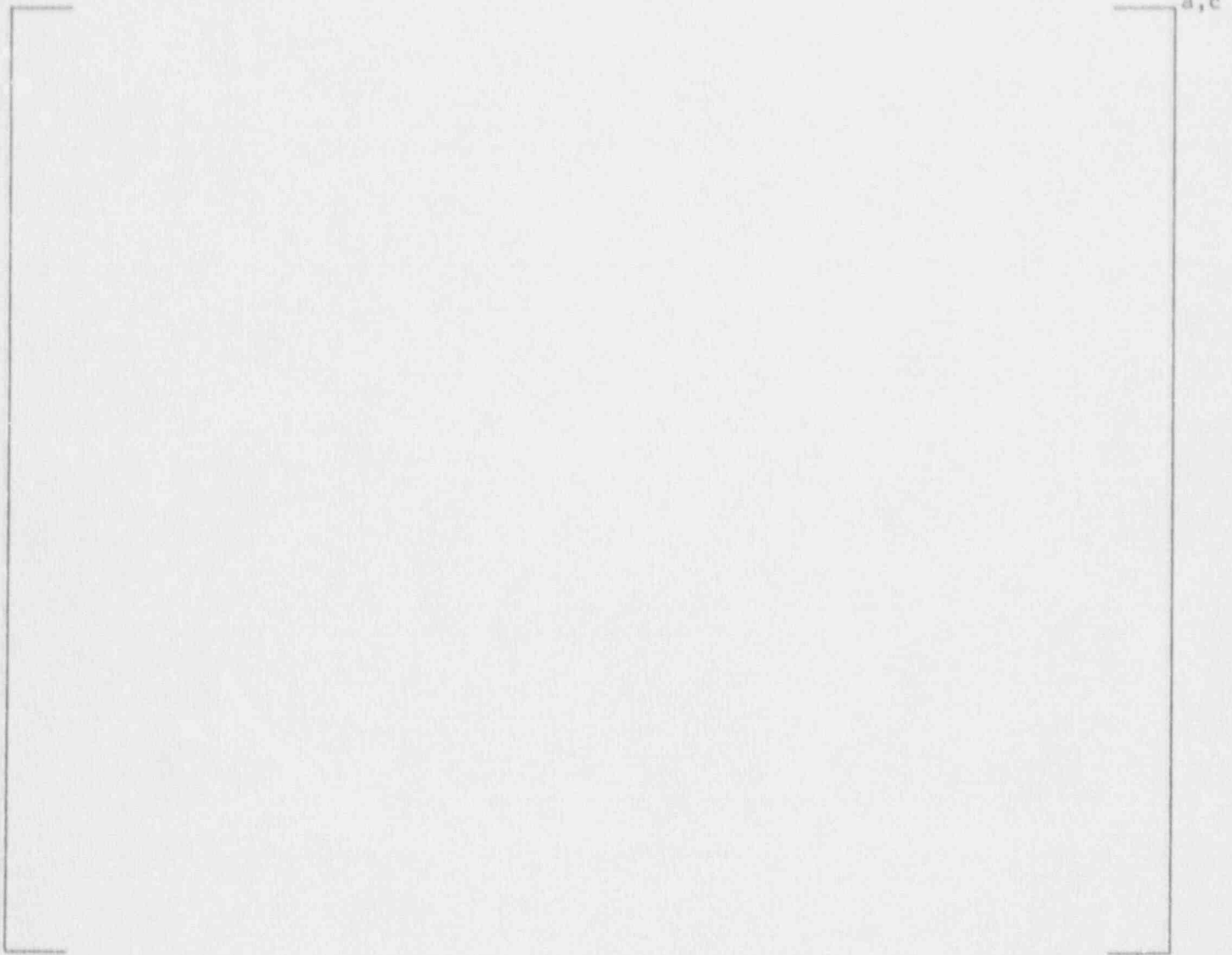


FIGURE 4.5.8 SEQUOYAH UNIT 2 CYCLE 5 LIMITING FQ
AT EACH AXIAL POINT
INC-5-F2-90-2A

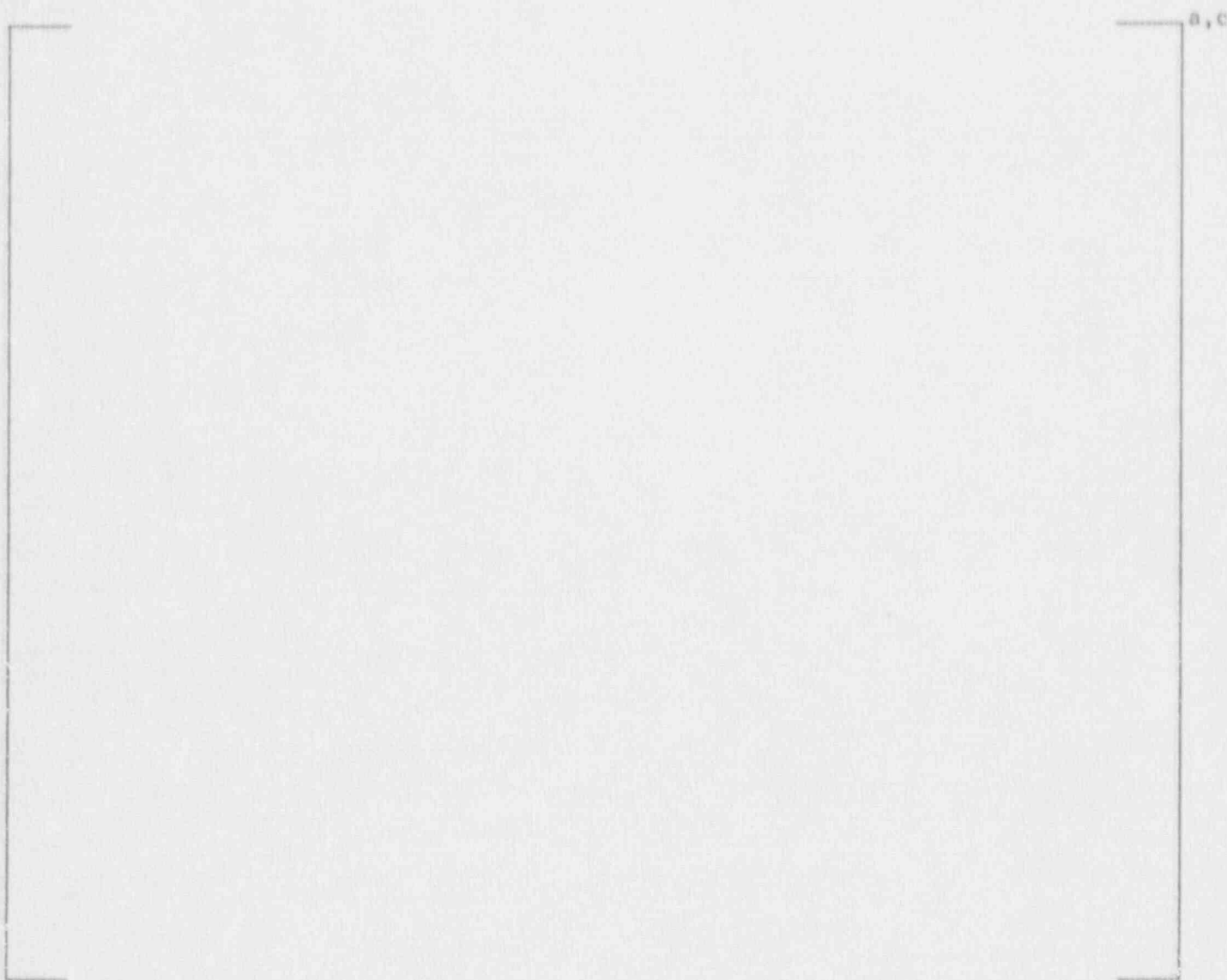
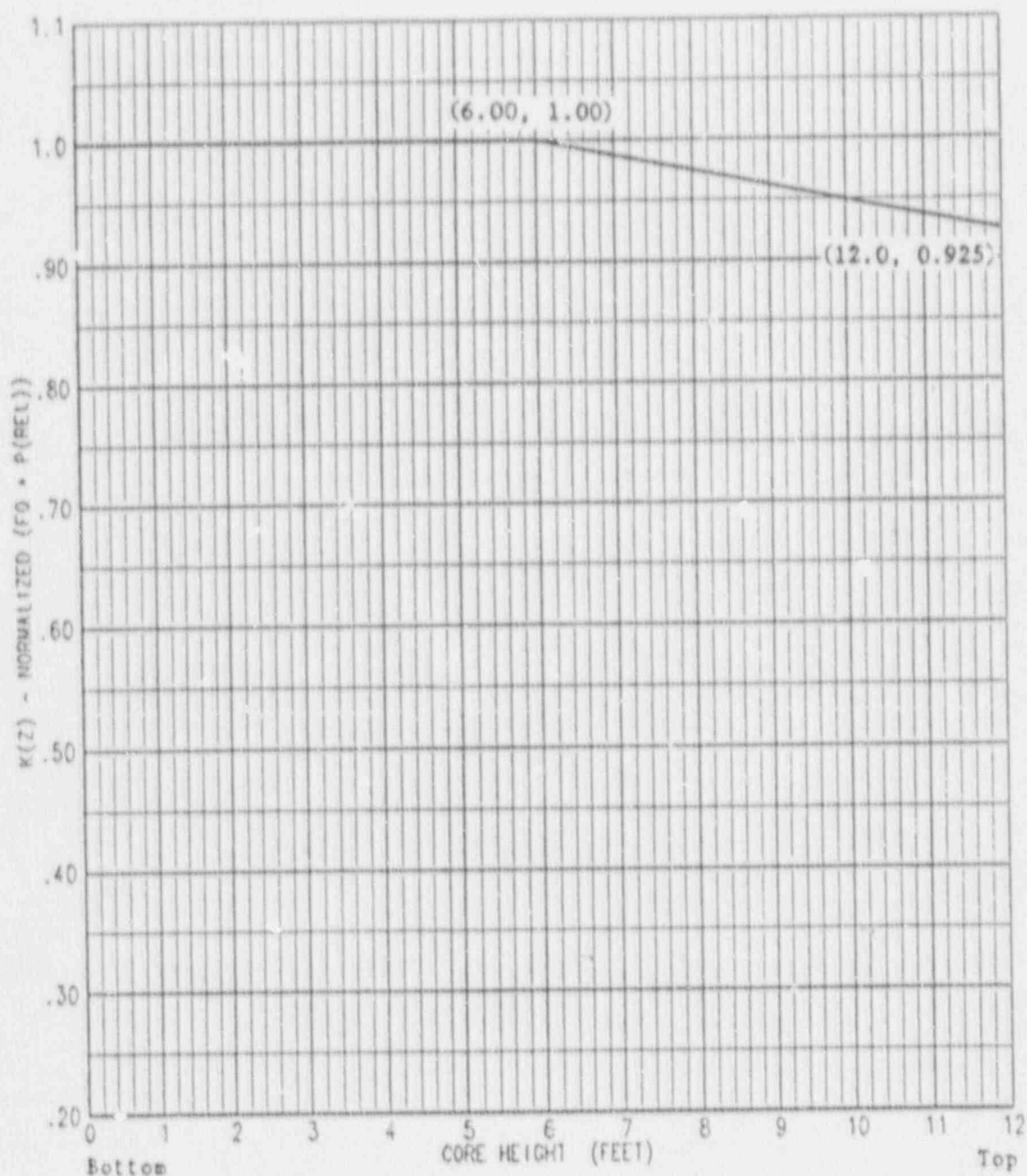


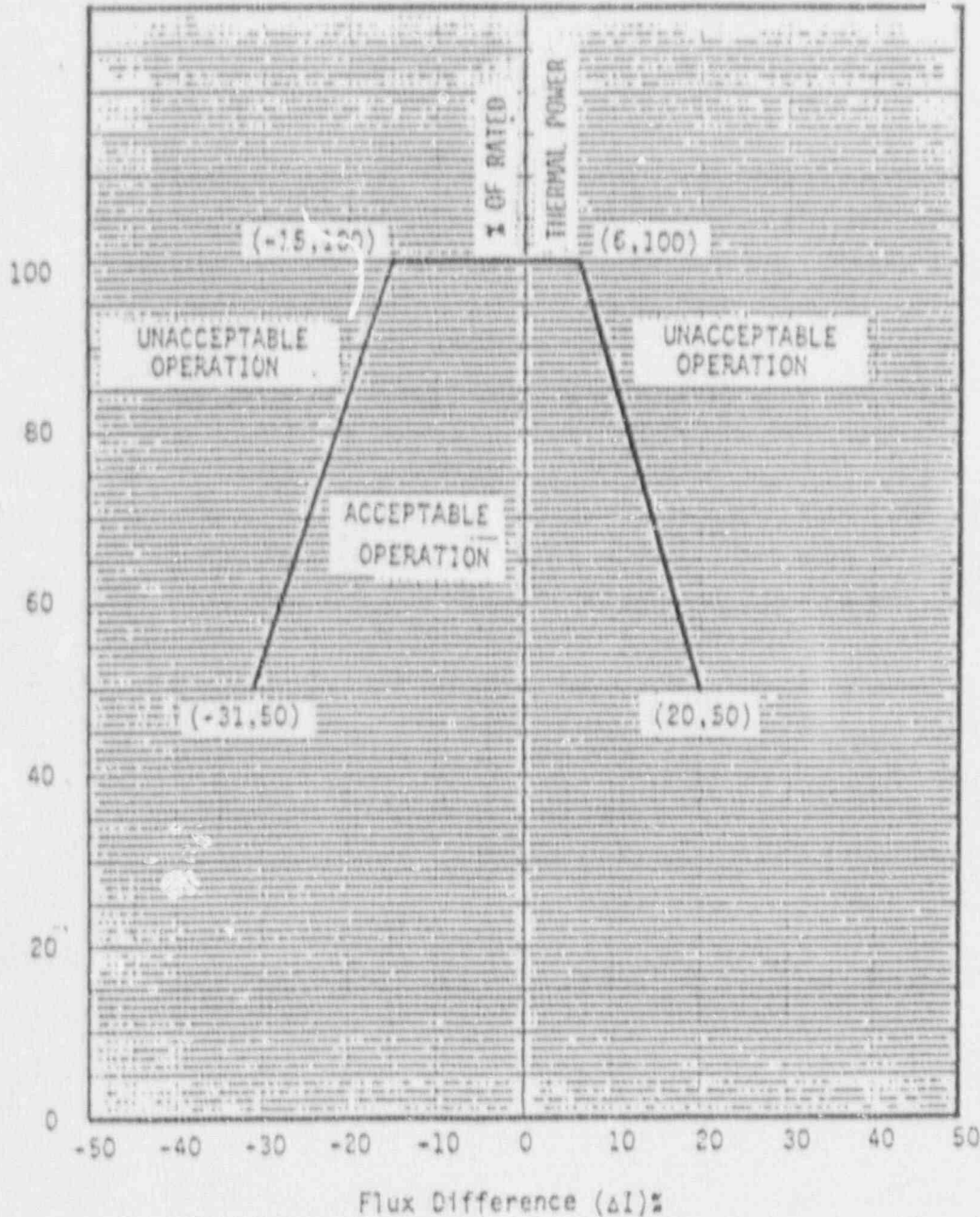
FIGURE 4.5.9 SEQUOYAH UNIT 2 CYCLE 5 LIMITING FQ,
AT EACH AXIAL POINT
INC-5-F2-90-11A

Figure 4.5.10



F_0 Normalized Operating Envelope, $K(Z)$ as a Function of Core Height

Figure 4.5.11



AXIAL FLUX DIFFERENCE LIMITS AS A FUNCTION OF RATED THERMAL POWER